We are IntechOpen,
the world's leading publisher of
Open Access books
Built by scientists, for scientists

6,900
Open access books available

185,000
International authors and editors

200M
Downloads

Our authors are among the

154
Countries delivered to

TOP 1%
most cited scientists

12.2%
Contributors from top 500 universities

CLARIVATE ANALYTICS
BOOK CITATION INDEX
INDEXED

WEB OF SCIENCE™

Selection of our books indexed in the Book Citation Index
in Web of Science™ Core Collection (BKCI)

Interested in publishing with us?
Contact book.department@intechopen.com

Numbers displayed above are based on latest data collected.
For more information visit www.intechopen.com

Chapter

Cartilage Tissue Engineering Using Self-Assembling Peptides Composite Scaffolds

Nausika Betriu and Carlos E. Semino

Abstract

Adult articular cartilage presents poor intrinsic capacity for regeneration, and after injury, cellular or biomaterial-based therapeutic platforms are required to assist repair promotion. Cartilage tissue engineering (CTE) aims to produce cartilage-like tissues that recreate the complex mechanical, biophysical and biological properties found *in vivo*. In terms of biomaterials used for CTE, three-dimensional (3D) self-assembling peptide scaffolds (SAPS) are very attractive for their unique properties, such as biocompatibility, optional possibility of rationally design cell-signaling capacity, biodegradability and modulation of its biomechanical properties. The most attractive cell types currently used for CTE are autologous chondrocytes and adult stem cells. The use of chondrocytes in cell-based therapies for cartilage lesions is limited by quantity and requires an *in vitro* 2D expansion, which leads to cell dedifferentiation. In the present chapter, we report the development of heparin-, chondroitin sulfate-, decorin-, and poly(ε-caprolactone)-based self-assembling peptide composite scaffolds to promote re-differentiation of expanded human articular chondrocytes and induction of adipose-derived stem cells to chondrogenic commitment.

Keywords: 3D cell culture, cartilage, self-assembling peptide scaffold, biomimetic materials, tissue engineering

1. Introduction

Articular cartilage is an avascular connective tissue, composed of chondrocytes as practically unique cell type. Articular chondrocytes synthesize, maintain and remodel the highly specialized extracellular matrix (ECM) [1], which in turn allows to withstand the mechanical requirements of the joints [2]. It is currently believed that due to its avascular nature, cartilage tissue lacks an intrinsic capacity for regeneration in response to disease or injury, leading to long-term pain, degeneration and loss of function [3]. Cartilage tissue engineering (CTE) aims to produce cartilage-like tissue substitutes by combining the appropriate cells, scaffolds and bioactive molecules to assist repair cartilage lesions [4, 5].

Cell types currently used for CTE include autologous articular chondrocytes (ACh), which already possess the desired phenotype, and mesenchymal stem cells (MSC), from bone marrow (BMSC) or adipose tissue-derived (ADSC), which can be induced to undergo chondrogenic differentiation [6, 7]. Autologous

chondrocytes would be the ideal cell source for cartilage repair due to their intrinsic properties regarding cell function and immune compatibility. However, cell accessibility from a patient biopsy is limited, and once isolated, chondrocytes needs to be extensively expanded in 2D monolayer [1]. During expansion process, chondrocytes rapidly undergo extensive loss of the original tissue-specific phenotype, downregulating the expression of chondrogenic markers, such as collagens and glycosaminoglycans while acquiring a fibroblast-like phenotype [8, 9].

Three-dimensional (3D) culture platforms are currently used to restore or maintain chondrogenic phenotype, since it recreates more closely the complex cellular microenvironment found *in vivo* [10, 11]. In terms of biomaterials used for CTE diverse possibilities in composition, structure, biodegradability and biomechanical properties exist. In general, biomaterials user for tissue engineering applications can be classified into natural or synthetic scaffolds. Natural scaffolds are commonly hydrogels made of natural materials such as Matrigel™, collagen type I, laminin and gelatin, which provide chemical cues, principally ECM binding motifs. However, due to its natural origin, they frequently contain undefined amounts of different constituents such as growth factors and cytokines which would be the main responsible of presenting variability from batch to batch [10]. Thus, due to its complex composition possible modifications to improve them are limited. On the other hand, synthetic scaffolds have minimal variation from batch to batch production, providing a reproducible cellular microenvironment. Moreover, they present lower biodegradability *in vitro*, fact that permits to maintain structural and mechanical properties for longer periods of time. Alike natural scaffolds, structural properties, such as matrix stiffness, can be modulated by increasing concentration. In the last decades, polymeric scaffolds, such as poly(lactic-co-glycolic acid) (PLGA) [12] and polylactic acid (PLA) [13, 14] as well as synthetic peptide nanofibers [15] have been developed to culture cells in 3D. Clinically used scaffolds are collagen type I/III and hyaluronic acid-based biomaterials, and others under consideration are for instance injectable fibrin gels, collagen type I or II and sponges, polylactic acid (PLA) and polyglycolic acid (PGA). As today, however, the best CTE product does not maintain their tissue properties after implantation, and the minimal medical standards are not yet achieved.

Synthetic hydrogels are good candidates for CTE since they possess unique properties, such as more than 95% of water content (which mimics the native cartilage ECM), biocompatibility and capacity of rationally design chemical signaling and biochemical properties. One of the best examples is the self-assembling peptide scaffold RAD16-I, commercially available as Puramatrix™. RAD16-I is a short peptide constituted by the sequence AcN-(RADA)$_4$-CONH$_2$, which alternates hydrophilic and hydrophobic amino acids (**Figure 1A**) [16]. The peptide undergoes self-assembly into a nanofiber network with antiparallel β-sheet configuration under physiological conditions (**Figure 1B**) [17]. The nanoscale architecture of the fiber network (around 10 nm diameter and 50–200 nm pore size) allows the cells to experiment a truly 3D environment (**Figure 1C**). Besides, biomolecules in such nanoscale environment diffuse slowly and are likely to establish a local molecular gradient. Non-covalent interactions allow cell growth, migration, contact with other cells, shape changes and a properly exposition of membrane receptors. Moreover, since stiffness can be controlled by changing peptide concentration these hydrogels can be tuned up to embed cells but not to entrap them [18].

Since the peptide scaffold does not contain signaling motifs, the environment can be considered non-instructive, from the point of view of cell receptor recognition/activation. However, the self-assembling peptide scaffold RAD16-I can be functionalized by solid-phase synthesis by extending at the N-termini with signaling motifs, such as ECM ligands for cell receptors, to trigger different cellular
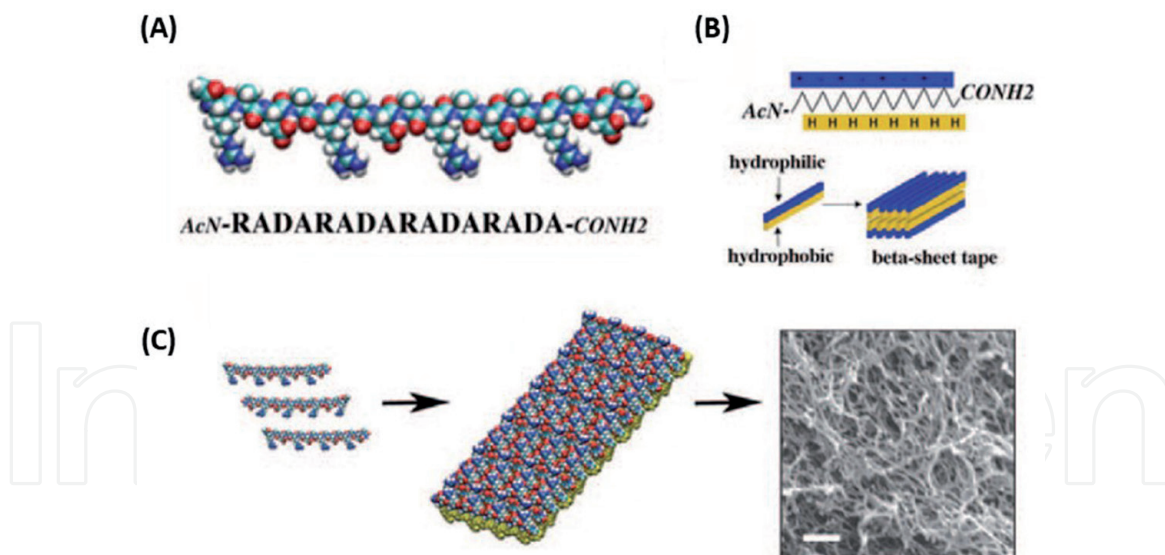
Figure 1.
Peptide RAD16-I self-assembles into a nanofiber network. (A) Molecular model of peptide RAD16-I. Since the scaffold contains no signaling moieties, the environment is not instructive for cells. R = Arg; A = Ala; D = Asp. (B) Molecular model of the nanofiber developed by self-assembling RAD16-I molecules. The nanofiber is formed by a double tape of assembled RAD16-I molecules in antiparallel β-sheet configuration. (C) RAD16-I nanofiber network viewed by SEM. The nanoscale architecture of the fiber network) allows the cells to experiment a truly 3D environment white bar represents 200 nm. Adapted from Semino [17].

responses [16, 19]. Several studies showed the capacity of RAD16-I to support cell maintenance of multiple cell types, including endothelial cells [20], hepatocytes [19, 21], fibroblasts [22], embryonic [23] and somatic stem cells [24, 25].

In the present chapter, we report the development of new bicomponent scaffolds based on the self-assembling peptide RAD16-I, for guiding chondrogenic differentiation of both adipose-derived stem cells (ADSC) and expanded dedifferentiated human articular chondrocytes (hACHs).

On one hand, we took advantage of the versatility of RAD16-I to specifically add molecular cues for guiding chondrogenesis in order to develop more biomimetic scaffolds. Thus, the first approach was based on the addition of heparin (Hep) moieties to the peptide scaffold, forming a stable electrostatic-based composite made of heparin-self-assembling peptide hydrogel. The advantage of this bicomponent scaffold is its natural capacity to retain heparin binding domain (HBD) containing growth factors (GFs), and thus, protecting them from degradation or denaturation [25]. Therefore, the non-instructive RAD16-I scaffold provides the structural 3D environment while the heparin moiety the binding structure to HBD-containing GFs. Our second approach, was based on mimicking the native articular cartilage ECM while providing signaling moieties presented in mature cartilage. Glycosaminoglycans (GAGs) and proteoglycans (PGs) are structural components of the native cartilage ECM and influence the regulation of cell proliferation, migration and differentiation [26]. In particular, chondroitin sulfate (CS, a sulfated GAG usually found as a constituent of PGs) and decorin (a small PG, consisting of a protein core linked to a GAG chain, consisting of chondroitin sulfate or dermatan sulfate) [27, 28] molecules were added to the RAD16-I scaffold by mixing the components, obtaining a chondroitin sulfate- and decorin-based self-assembling peptide composite scaffold.

Finally, we combined the self-assembling peptide RAD16-I with a woven poly (ε-caprolactone) (PCL). 3D weaving can be used to create porous structures arranged in multiple layers of continuous fibers in three orthogonal directions [29]. Such scaffolds were engineered with predetermined properties aiming to reproduce the mechanical features of native articular cartilage. Moreover, PCL is a Food and Drug

Administration (FDA) approved biomaterial, biocompatible and biodegradable, widely used for medical applications [30, 31]. Our strategy was based on combine these two biomaterials to promote the attachment and differentiation of embedded cells, providing at the same time a biomimetic mechanical environment of the native mature cartilage [32].

2. Materials and methods

2.1 2D culture of ADSC and hACh

ADSC (PT-5006, Lonza) were cultured in 175 cm^2 T-flasks (<6th passage) in Adipose-Derived Stem Cell Basal Medium (ADSC-BM) (PT-3273, Lonza) supplemented with Adipose-Derived Stem Cell Growth Medium (ADSC-GM) SingleQuots (PT-4503, Lonza). hACh cells (CC-2550, Lonza) were cultured at 10,000 cells/cm^2 from passages 2–6 in 25, 75, and 175 cm^2 T flasks. The growth medium consisted of Chondrocyte Basal Medium (CBM) (CC-3217, Lonza) plus SingleQuots of Growth Supplements (CC-4409, Lonza) containing R3-IGF-1, bFGF, transferrin, insulin, FBS, and gentamicin/amphotericin-B. Cultures were maintained in the incubator in humidified atmosphere at 37°C and 5% CO_2.

2.2 3D culture of ADSC and hACh in RAD16-I composites scaffolds

ADSC and hACh 3D cultures were maintained under control or chondrogenic conditions. Control medium was prepared with DMEM High Glucose, GlutaMAX (61965, Gibco), ITS + Premix 100x (354352, BDBioscience), 100 U/mL Penicillin/100 μg/mL Streptomycin (P11-010, PAA), 40 μg/mL L-Proline (P5607, Sigma) and 1 mM Sodium Pyruvate (11360, Life Technologies). Cultures for chondrogenic differentiation were induced at day 2 with chondrogenic medium (control medium supplemented with 10 ng/mL TGFβ1 (GF111, Millipore), 25 μg/mL L-ascorbic acid 2-phosphate (A8960; Sigma) and 100 nM Dexamethasone (D8893; Sigma)). Chondrocytes were also cultured in expansion medium (see Section 2.1). 3D cell cultures were maintained in the incubator at 37°C and 5% CO_2, and medium was changed every other day. Cultures were maintained for 4 weeks in the described serum-free media under control or chondrogenic conditions (in the presence of stimulating factors to induce chondrogenic differentiation) [33, 34]. After 4 weeks, 3D constructs were analyzed for morphology, gene and protein expression, glycosaminoglycans production and mechanical properties.

2.3 ADSC 3D culture in RAD/heparin composite scaffold

RAD16-I (PuraMatrix™, 354250, Corning) and composites RAD/Hep were prepared at a final concentration of 0.3% (w/v) RAD16-I. The composites were prepared by combining 95 μL of 0.5% (w/v) RAD16-I and 5 μL of heparin sodium salt solution (H3149, Sigma) in a concentration range between 0.01% and 1% (w/v). The mixture was then diluted with 10% sucrose (S0389, Sigma) to a final concentration of 0.3% (w/v) RAD16-I. To obtain RAD and RAD/Hep 3D cultures, ADSC were harvested by trypsinization and resuspended to 4 × 10^6 cells/mL in 10% sucrose. The 0.3% (w/v) RAD16-I peptide solution was mixed with the cell suspension (1:1) to obtain a final concentration of 0.15% (w/v) RAD16-I and 2 × 10^6 cells/mL. Then, 80 μL of the cell-peptide mixture (160,000 cells) was loaded into individual wells of a 48-well culture containing 150 μL of medium, which induced the self-assembly of the peptide. The plate was placed in the incubator for 20 min

at 37°C and 5% CO_2, and then 650 μL of fresh medium was added to the 3D cell cultures. ADSC 3D cultures were maintained during 2 days under control medium. Cultures for chondrogenic differentiation were induced at day 2 with chondrogenic medium.

2.3.1 ADSC and hACh 3D culture in RAD/CS and RAD/Dec composite scaffold

RAD16-I (PuraMatrix™, 354250, Corning) and composites RAD/CS and RAD/Decorin were prepared at a final concentration of 0.3% (w/v) RAD16-I. The composites were prepared by combining 95 μL of 0.5% (w/v) RAD16-I and 5 μL CS or Decorin at a concentration of 0.2% (w/v). The mixture was then diluted with 10% sucrose (S0389, Sigma) to a final concentration of 0.3% (w/v) RAD16-I. To obtain RAD16-I, RAD/CS and RAD/Decorin 3D cultures, cells were harvested by trypsinization and resuspended to 4×10^6 cells/mL in 10% sucrose. The 0.3% (w/v) RAD16-I peptide solution was mixed with the cell suspension (1:1) to obtain a final concentration of 0.15% (w/v) RAD16-I and 2×10^6 cells/mL. Then, 80 μL of the cell-peptide mixture (160,000 cells) was loaded into individual wells of a 48-well culture containing 150 μL of control or expansion medium, which induced the self-assembly of the peptide. The plate was placed in the incubator for 20 min at 37°C and 5% CO_2, and then 650 μL of fresh medium was added to the 3D cell cultures.

2.3.2 hACh 3D culture in PCL, PCL/RAD and RAD scaffolds

In the case of PCL scaffold, a cell suspension of 25×10^6 cells/mL was seeded onto the surface of 5 mm × 0.75 mm woven PCL scaffolds (500,000 cells/scaffold). After 2 h, 100 μL of expansion or control medium were slowly added into the well and after 4 h, 700 μL were finally added. For PCL/RAD composites, cells were harvested and resuspended to 50×10^6 cells/mL in 10% (w/v) sucrose. Then, cells were equally mixed with 1% (w/v) RAD16-I and seeded onto the woven PCL scaffold disks (500,000 cells/scaffold). Then, 40 μL of expansion or control medium was added and the gel was spontaneously formed inside the PCL scaffolds, where the cells were embedded. After 30 min, 60 μL of medium was added in the well, and after 2 h, 700 μL was finally added. 3D cell cultures were maintained in the incubator at 37°C and 5% CO_2, and medium was changed every other day.

3. Representative results

Autologous chondrocytes are one of the most attractive cell types for CTE, due to their intrinsic properties regarding cell function, since they are found in the native cartilage. Chondrocytes are characterized by a rounded morphology, the production of tissue-specific ECM components such as collagen type I and II and glycosaminoglycans (GAGs). One of the main challenges in CTE is to obtain enough cell mass to develop a tissue construct with the desirable biological and biomechanical properties. Particularly, articular chondrocytes are obtained by invasive techniques and cell number in patient biopsies is limited. Therefore, after isolation, chondrocytes need to be expanded in 2D monolayer [1]. The expansion process leads to a rapid downregulation of chondrogenic markers, such as Collagen type I (COL1) collagen type II (COL2) and Aggrecan (ACAN) [8, 9]. Moreover, the use of extensively passaged cells leads to some degree of hypertrophy, decreased biochemical content and compromised mechanical properties [1], which is not a good indication for cartilage substitute applications.

Mesenchymal stem cells (MSCs) have generated great interest as an alternative cell source to autologous chondrocytes. MSCs are pluripotent cells with a high proliferative capacity that can be differentiated, under the appropriate microenvironment, to numerous cell lineages, such as osteogenic, adipogenic and chondrogenic [35]. MSCs can be isolated from bone marrow, adipose tissue and other sources. In particular, the adipose tissue provides and abundant reservoir of mesenchymal stem cells (adipose-derived stem cells, ADSC), which can be obtained by non-invasive surgical techniques. ADSC can undergo chondrogenic commitment in the presence of TGF-β, ascorbate, and dexamethasone combined with a 3D culture environment [35].

Three-dimensional scaffold-based cell cultures are currently used in CTE to reestablish chondrogenic phenotype of dedifferentiated chondrocytes, since they mimic more closely the natural tissue environment. On the other hand, differentiation of ADSC to cartilage-like tissue has been achieved in various 3D scaffold systems such as alginate [36], agarose [37] and collagen [38]. We report here the development of new bicomponent scaffolds based on the self-assembling peptide RAD16-I, for guiding chondrogenic differentiation of both adipose-derived stem cells (ADSC) and expanded dedifferentiated human articular chondrocytes (hAChs).

3.1 Bicomponent scaffolds made out of heparin/self-assembling peptide hydrogels

In this section, we report the development of a nanofiber scaffold with growth factor binding affinity. The strategy consisted of adding heparin moieties to the RAD16-I peptide scaffold by mixing the two components, forming a stable composite hydrogel scaffold with a natural capacity to retain HBD-containing growth factors. To evaluate the functionality of this approach for CTE applications, ADSC were cultured in the new bicomponent scaffold and induced to chondrogenic differentiation using TGFβ-1, L-ascorbic acid 2-phosphate and dexamethasone as inductors in serum-free media. 3D cultures were maintained for 4 weeks in chondrogenic or control medium, and analyzed for proteoglycan production, protein expression and mechanical properties.

During ADSC culture in the peptide scaffold RAD16-I combined with increasing concentrations of heparin (RAD/Hep), constructs cultured under chondrogenic medium—unlike constructs under control medium—became highly stained with toluidine blue, indicating a significant production of proteoglycans (**Figure 2A**). This result correlated with the aggrecan (*ACAN*) gene expression, which was only detected in constructs under chondrogenic induction (**Figure 2B**). ADSC cultured within RAD/Hep composites also produced cartilage-specific ECM proteins, such as COL1, COL2 and COL10 (**Figure 2C**). Interestingly, a single band was obtained for COL1 in 2D culture, corresponding probably to a pro-collagen intermediate (approx. 220 kDa). Different bands (ranging from 130 to 180 kDa) were obtained for COL1 in 3D constructs under chondrogenic induction. Importantly, COL2 was only detected in 3D chondro-induced cultures.

Moreover, mechanical characterization was performed over 3D chondro-induced constructs. 3D constructs, presented a storage modulus (G′) in the same order of magnitude to chicken or calf articular cartilage, but the full mechanical response of the constructs was different from native cartilage as evidenced by tan(delta) (**Figure 2D**).

3.2 Bicomponent scaffolds made out of chondroitin sulfate or decorin and self-assembling peptide hydrogels

The next strategy was based on mimicking the native cartilage ECM by adding chondroitin sulfate or decorin molecules to the nanofiber scaffold, generating thus
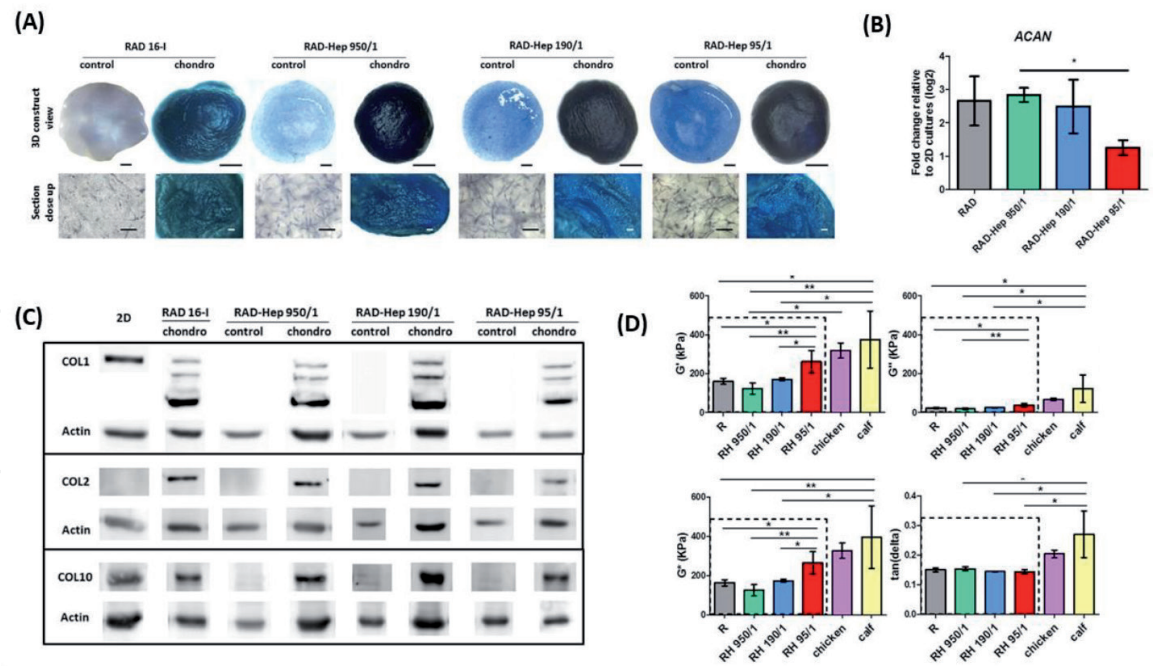
Figure 2.
Chondrogenic capacity of ADSC in RAD/heparin composite scaffold. ADSC were encapsulated within the RAD16-I peptide scaffold combined with increasing concentrations of heparin and cultured for 4 weeks under control and chondrogenic medium. (A) Toluidine blue staining of 3D ADSC constructs cultured under control and chondrogenic medium. 3D construct view scale bars = 500 μm and section close up scale bars = 100 μm. (B) Aggrecan gene expression levels of chondro-induced ADSC. Constructs cultured with control medium did not express aggrecan after 4 weeks of culture. Ct values relative to ribosomal protein L22 (RPL22) were obtained and reported as fold increase (ΔΔCt) relative to 2D cultures. (C) Protein expression characterization of ADSC cultured in RAD/Hep composites and in 2D monolayer. Western blot results of collagen type I, II and X when ADSC were maintained in control and chondrogenic medium in RAD16-I scaffold and RAD16-I/Hep composites. Actin expression was used as an internal control. (D) Mechanical characterization of 3D constructs cultured for 4 weeks in chondrogenic medium compared to chicken and calf articular cartilage. ADSCs cultured with RAD16-I and RAD/Hep composite scaffolds were analyzed for storage modulus (G', A), loss modulus (G'', B), complex modulus (G, C) and tan(delta). Significant differences are indicated as * for p < 0.05, ** for p < 0.01, and *** for p < 0.001, one-way ANOVA, N = 2 n = 3). Adapted from Fernández-Muiños et al. [25].*

chondro-favorable biochemical cues in the 3D environment. Previous work has evaluated the influence of CS to guide chondrogenesis in different hydrogel scaffolds such as chitosan [39], PEG [40], or collagen type I [41], but less is known about the ability of decorin to promote chondrogenesis commitment. In the present work, we studied the influence of both CS and decorin molecules on chondrogenesis in a nanometric 3D system. The capacity of these bicomponent scaffolds to foster chondrogenic differentiation was evaluated in two different scenarios: re-differentiation of expanded hAChs and induction of ADSC to chondrogenic commitment. Cells were seeded in RAD16-I/CS, RAD16-I/Dec and RAD16-I scaffold alone and maintained for 4 weeks in chondrogenic or control medium. Moreover, chondrocytes were also cultured in expansion medium, which contains GFs that could affect the fate of the 3D culture. 3D constructs were analyzed for morphology, gene and protein expression, proteoglycan synthesis and mechanical properties.

SEM images were obtained at week 4 of culture to assess cell morphology and their interaction with each scaffold (**Figure 3**). Articular chondrocytes cultured in expansion medium possessed a spherical morphology with possible cell-matrix interactions and thorough ECM components. Nanofibers and putative matrix components were detected on the surface of constructs cultured in control medium. Moreover, grooves with visible fibers were observed on the surface of constructs cultured in chondrogenic medium, fact that suggested the presence of secreted matrix components. On the other hand, adipose-derived stem cells under chondrogenic induction looked elongated and anchored to the scaffold surface, while
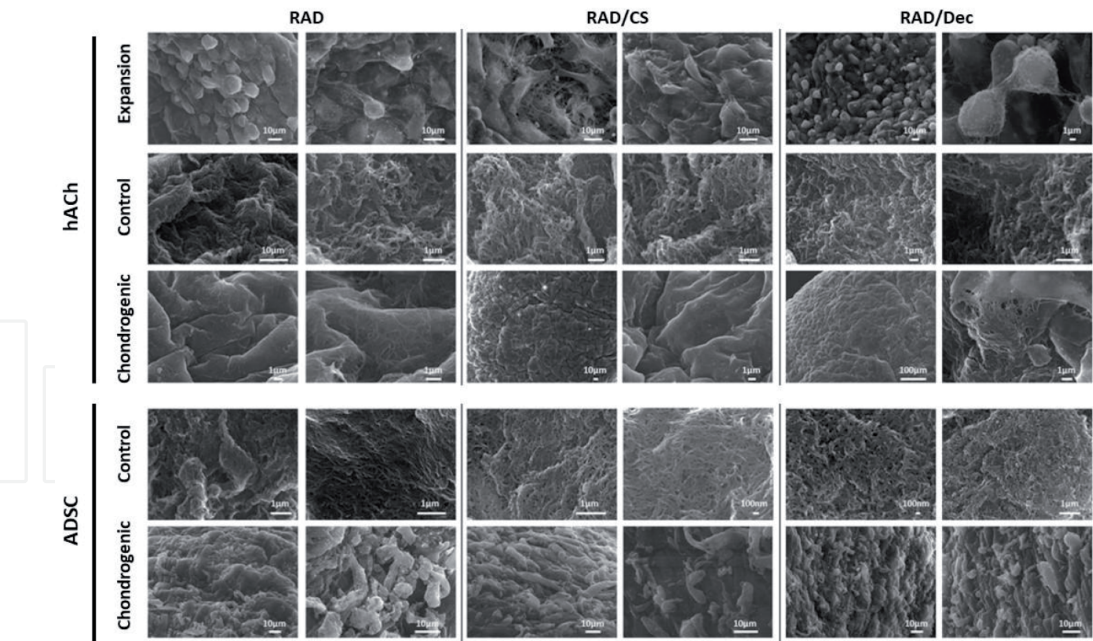
Figure 3.
SEM images of hACh and ADSC at week 4 of culture in RAD, RAD/CS and RAD/Dec scaffolds. Two images per condition are shown. Adapted from Recha-Sancho and Semino [42].

nanofibers and possible ECM components synthesized by the cells were observed in control medium (**Figure 3**). No significant differences in cell morphology were detected between RAD, RAD/CS or RAD/Dec scaffolds in any cell type.

Chondrogenic markers expression were studied at gene and protein level in hACh 3D constructs cultured in chondrogenic and expansion medium, and compared to their 2D counterparts. *COL1* was upregulated in all 3D scaffolds under chondrogenic medium and downregulated under expansion medium (**Figure 4A**). At protein level, COL1, was detected both in 2D monolayer and 3D constructs, but different band patterns were observed (**Figure 4B**). In 2D cultures, a single band was detected (approx. 220 kDa), generated probably by a pro-collagen intermediate. In 3D cultures, different bands of lower molecular weight (ranging from 130 to 180 kDa) were observed, but their intensity varied depending on the culture medium.

Interestingly, *COL2* gene expression was only upregulated in RAD/CS and RAD/Dec composite scaffolds under chondrogenic medium. This result correlated with the expression of *SOX9*, a gene regulator of *COL2*, which was significantly upregulated in 3D constructs under chondrogenic induction (**Figure 4A**). At protein level, COL2 was only detected in 3D cultures under chondrogenic induction, fact that was consistent with the gene expression profile results (**Figure 4B**). *ACAN* gene expression was higher in constructs under chondrogenic medium than in constructs cultured under expansion medium (**Figure 4A**). No differences were detected in the gene expression of hypertrophic markers compared to 2D cultures, except in RAD16-I scaffold alone, where the expression of *COL10* was upregulated in expansion medium, and *RUNX2* in chondrogenic medium (**Figure 4A**). COL10 protein expression was observed in all conditions, including 2D, but more intense bands were detected in expansion and chondrogenic medium, compared to control (**Figure 4B**).

Toluidine blue staining was performed in hACh 3D constructs to qualitatively assess the production of GAGs. Constructs under chondrogenic induction became highly stained, indicating a significant production and accumulation of GAGs by the cells (**Figure 4C**). Constructs cultured under expansion medium showed less staining, while constructs under control medium became weakly stained.
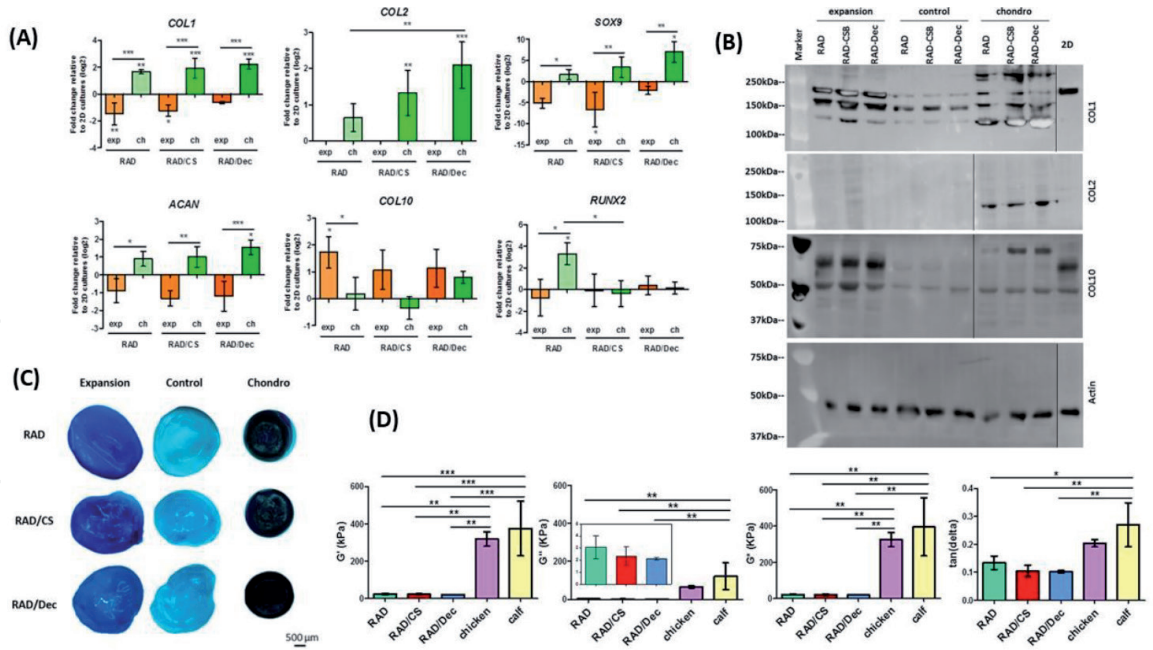
Figure 4.
Chondrogenic capacity of dedifferentiated hACh in RAD/CS and RAD/Dec 3D composite scaffolds. hACh were encapsulated within the RAD16-I peptide scaffold combined with chondroitin sulfate and decorin, and cultured for 4 weeks under expansion, control and chondrogenic medium. (A) Gene expression levels of chondrogenic and hypertrophic markers. hACh were analyzed by qRT-PCR for collagen type I (COL1), collagen type II (COL2), SOX9, aggrecan (ACAN), collagen type X (COL10) and RUNX2. Ct values relative to ribosomal protein L22 (RPL22) were obtained and reported as the fold increase (ΔΔCt) relative to 2D cultures (B) protein expression characterization of hACh cultured in RAD, RAD/CS and RAD/Dec composites and in 2D monolayer. Western blot results of collagen type I (COL1), II (COL2) and X (COL10) when hACh were maintained in expansion, control and chondrogenic media in the different scaffolds (RAD, RAD/CS and RAD/Dec) and in 2D monolayer. Actin expression was used as an internal control. Samples were prepared in triplicate. (C) Toluidine blue staining of hACh 3D RAD, RAD/CS and RAD/Dec constructs cultured in expansion, control and chondrogenic medium. Proteoglycan synthesis was qualitatively assessed by toluidine blue staining. (D) Mechanical characterization of 3D constructs cultured for 4 weeks in chondrogenic medium compared to chicken and calf articular cartilage. hACh cultured with RAD16-I and RAD/CS and RAD/Dec composite scaffolds were analyzed for storage modulus (G′), loss modulus (G″), complex modulus (G*) and tan(delta). Significant differences are indicated as * for p < 0.05, ** for p < 0.01, and *** for p < 0.001, one-way ANOVA, N = 2 n = 3). Adapted from Recha-Sancho and Semino [42].

The mechanical properties of hACh 3D constructs cultured under chondrogenic medium were assessed at week 4 by dynamic mechanical analysis (DMA) and compared to calf and chicken articular cartilage (**Figure 4D**). hACh constructs exhibited lower storage modulus values (G′) than did the native cartilage samples. The viscous components (G″) and the complex modulus (G*) displayed a more similar tendency to cartilage controls. Nevertheless, all samples presented G′ values higher than G″ values, indicating that the constructs were more elastic than viscous. Tan(delta) showed that 3D constructs were comparable to chicken cartilage but differed from calf cartilage.

Chondrogenic and hypertrophic markers were studied in ADSC 3D constructs in the three scaffold types and compared to 2D monolayer culture. Results show that the gene expression of *COL1* was downregulated in 3D cultures. However, the expression of *COL2*, *SOX9* and *ACAN* was increased in 3D cultures compared to 2D. The expression levels of the hypertrophic markers *COL10* and *RUNX2* in 3D cultures were maintained at comparable levels to 2D culture (**Figure 5A**). At protein level, ADSC under chondrogenic induction produced cartilage-specific ECM proteins such as COL1, COL2 and COL10 (**Figure 5B**). As happened for hACh, one single band was obtained for *COL1* in 2D monolayer, while different bands of lower molecular weight were observed in 3D cultures. Interestingly, COL2 protein was only detected in 3D cultures.

Chondro-induced ADSC produced sulfated glycosaminoglycans, as reveals the intense staining by toluidine blue (**Figure 5C**, up). No calcium mineralization, an indicator of hypertrophy, was detected by Von Kossa staining (**Figure 5C**, down).

The mechanical properties of ADSC cultured under chondrogenic conditions in RAD, RAD/CS and RAD/Dec were assessed by dynamic mechanical analysis (DMA) at week 4 (**Figure 5D**). The constructs presented a storage modulus (G′), viscous component (G″) and complex modulus (G*) closely related to chicken and calf cartilage. However, samples presented values of G′ much higher than G′′ so that the constructs were more elastic than viscous. Tan(delta) showed that the full mechanical response of the constructs was very similar to chicken cartilage but differed from calf cartilage.

In the present work, we aimed to induce chondrogenesis differentiation of both expanded hACh and ADSC in 3D bicomponent scaffolds made out of chondroitin sulfate or decorin and self-assembling peptide hydrogels. The expression of chondrogenic markers such as *COL2*, *SOX9* and *ACAN* was increased in both cell types compared to monolayer cultures (**Figures 4A** and **5A**). At protein level, western blot results showed a possible COL1 maturation process in 3D cultures of both cell types compared to 2D protein expression. In particular, the final mature COL1 product corresponds to the lower molecular weight band (130 kDa), which was absent in 2D cultures but predominant in constructs under chondrogenic medium (**Figures 4B** and **5B**). Importantly,
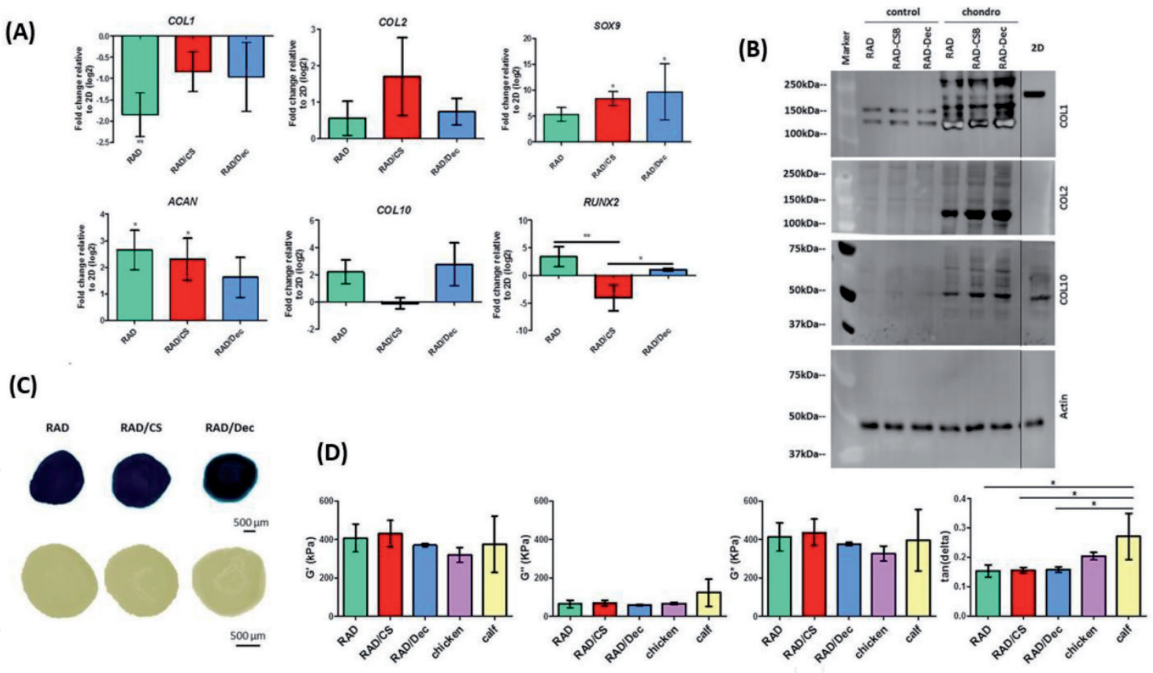

Figure 5.
Chondrogenic capacity of ADSC in RAD/CS and RAD/Dec 3D composite scaffolds. ADSC were encapsulated within the RAD, RAD/CS and RAD/Dec composite scaffolds and cultured for 4 weeks under control and chondrogenic medium. (A) Gene expression levels of chondrogenic and hypertrophic markers. ADSC were analyzed by qRT-PCR for collagen type I (COL1), collagen type II (COL2), SOX9, aggrecan (ACAN), collagen type X (COL10) and RUNX2. Ct values relative to ribosomal protein L22 (RPL22) were obtained and reported as the fold increase (ΔΔCt) relative to 2D cultures. (B) Protein expression characterization of ADSC cultured in RAD, RAD/CS and RAD/Dec composites and in 2D monolayer. Western blot results of collagen type I (COL1), II (COL2) and X (COL10) when ADSC were cultured under control and chondrogenic medium in the different scaffold types. Actin expression was used as an internal control. (C) Toluidine blue and Von Kossa staining of 3D ADSC constructs under chondrogenic induction. Proteoglycan synthesis was qualitatively assessed by toluidine blue staining (up) and calcium mineralization by Von Kossa staining (down). (D) Mechanical characterization of 3D constructs cultured for 4 weeks in chondrogenic medium compared to chicken and calf articular cartilage. ADSCs cultured with RAD16-I and RAD/CS and RAD/Dec composite scaffolds were analyzed for storage modulus (G', A), loss modulus (G'', B), complex modulus (G, C) and tan(delta). Significant differences are indicated as * for p < 0.05, ** for p < 0.01, and *** for p < 0.001, one-way ANOVA, N = 2 n = 3). Adapted from Recha-Sancho and Semino [42].*

COL2 expression was only detected in 3D cultures under chondrogenic induction. Moreover, GAG production and accumulation was confirmed by toluidine blue staining (**Figures 4C** and **5C**). Altogether, these results indicate the synergistic effect of the 3D culture system and the chemical inducers present in the chondrogenic medium in activating signaling pathways essentials for chondrogenic commitment, in terms of production of proteins and GAG components of the ECM. Finally, mechanical characterization showed that the viscoelastic behavior of chondro-induced ADSC constructs was more similar to native cartilage than hACh constructs (**Figures 4D** and **5D**). In resume, results until this section clearly indicate the chondro-inductive capacity of the modified scaffold which reinforce the development of biomimetic microenvironments to promote better tissue engineered cartilage substitutes.

3.3 Bicomponent scaffolds made out of PCL and self-assembling peptide hydrogels

Self-assembling peptide hydrogels provide a soft and permissive microenvironment, allowing cells to migrate, extend cellular processes and contact with other cells. Nevertheless, the use of soft hydrogels for CTE can be challenging due to its low stiffness. One approach to address this issue is the use of composite scaffolds, comprising a microscale component to increase mechanical properties and a hydrogel component (of nanoscale dimension) to promote chondrogenesis. Woven 3D poly(ε-caprolactone) (PCL) resemble native cartilage mechanical properties and, due to its high wettability, can be infiltrated with a hydrogel matrix, such as fibrin, alginate, and poly-acrylamide [43–45]. In this study, we developed a unique composite scaffold by infiltrating a 3D woven microfiber poly(ε-caprolactone) scaffold with the RAD16-I self-assembling peptide nanofiber to obtain a multi-scale functional cartilage-like tissue. The chondrogenic capacity of this new bicomponent was evaluated with expanded dedifferentiated human articular chondrocytes.

The high wettability properties of the PCL scaffold (**Figure 6A**) allowed to easily introduce the cells suspended in the RAD16-I peptide solution between the
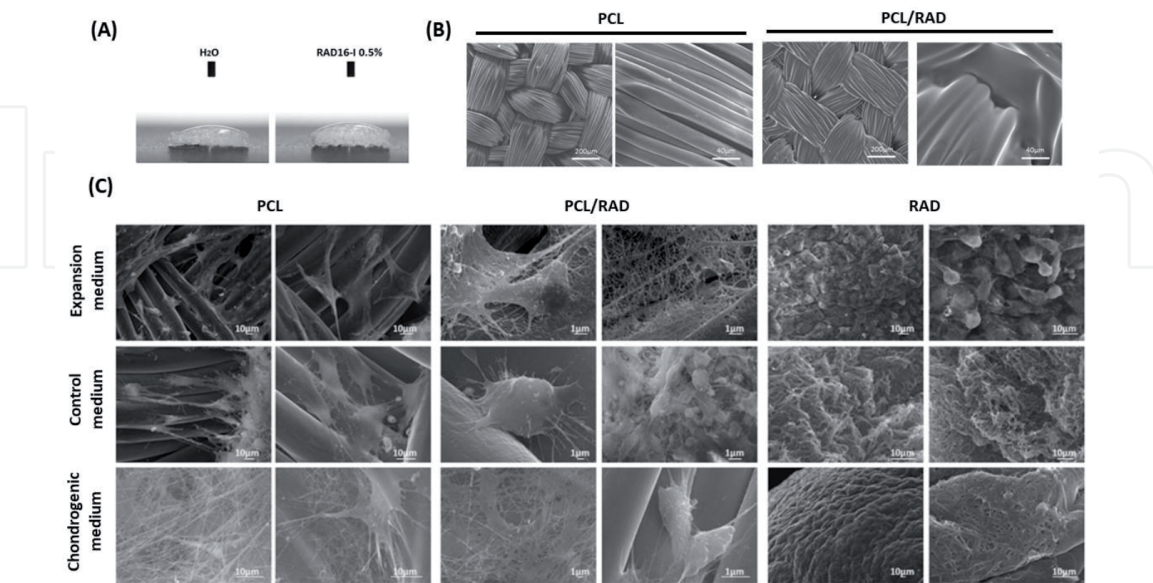

Figure 6.
SEM characterization of PCL/RAD and hACh constructs. (A) Water (left) and 0.5% RAD16-I solution (right) contact angle. The liquid was totally absorbed by the PCL scaffold (contact angle << 90°), indicating high wettability. (B) Surface view of PCL and PCL/RAD structure by SEM. 0.5% RAD16-I was lyophilized within the PCL scaffold. (C) hACh at week 4 of culture in PCL, PCL/RAD and RAD scaffolds. hACh were seeded in each scaffold and cultured in expansion, control and chondrogenic medium. Two images per condition are shown. Adapted from Recha-Sancho et al. [46].

interweaving fibers of PCL scaffold (**Figure 6B**, left). Areas of RAD16-I peptide deposition could be observed within the organized woven morphology of the fiber scaffold (**Figure 6B**, right). Thus, cells were seeded in the composite PCL/RAD and in the two scaffolds independently, PCL and RAD, and maintained for 4 weeks in expansion, chondrogenic and control medium. 3D constructs were analyzed for morphology, gene and protein expression, proteoglycan synthesis and mechanical properties.

In order to evaluate cell morphology and their interaction with the scaffolds, SEM images of hACh cultured in PCL, PCL/RAD and RAD 3D scaffolds in expansion, control and chondrogenic medium were taken at week 4 of culture (**Figure 6C**). hACh seeded in PCL scaffolds looked elongated and growing on the surface of PCL fibers. Interestingly, more fibers were detected under chondrogenic induction, probably due to an increase in extracellular matrix components production by the cells. In PCL/RAD constructs, cells seemed to be attached to the PCL fibers, with a more spherical morphology than in PCL scaffold alone, while hACh in RAD scaffolds presented in general a spherical shape.

Chondrogenic and hypertrophic markers were studied at gene and protein level at week 4 of culture in 3D scaffolds and compared to 2D cultures. *COL1* was downregulated or maintained at 2D culture levels under expansion medium, while it increased in all 3D constructs under chondrogenic conditions (**Figure 7A**). At protein level a single band (~220 kDa) was obtained for COL1 in 2D culture, while different bands of lower molecular weight (ranging from 180 to 130 kDa) were observed in 3D cultures of PCL/RAD and RAD (in all medium tested) and PCL in chondrogenic conditions (**Figure 7B**).

The expression of *COL2* was only increased in PCL/RAD and PCL scaffolds under chondrogenic induction, however, significant differences were only detected
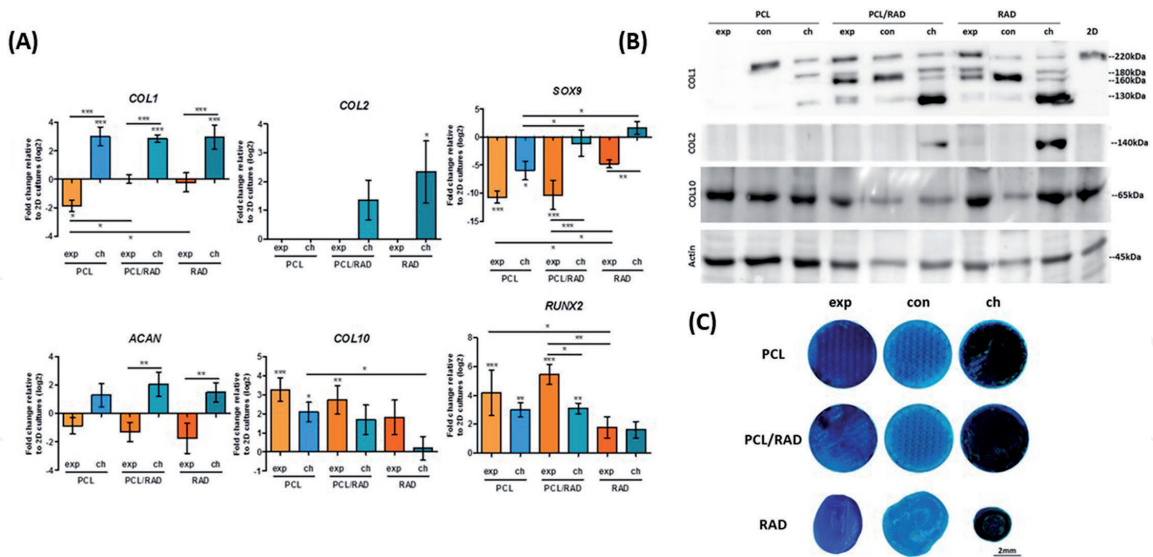

Figure 7.
Chondrogenic capacity of dedifferentiated hACh in PCL, PCL/RAD and RAD scaffolds. hACh were seeded in each scaffold, and cultured for 4 weeks under expansion, control and chondrogenic medium. (A) Gene expression levels of chondrogenic and hypertrophic markers. hACh were analyzed by qRT-PCR for collagen type I (COL1), collagen type II (COL2), SOX9, aggrecan (ACAN), collagen type X (COL10) and RUNX2. Ct values relative to ribosomal protein L22 (RPL22) were obtained and reported as the fold increase (ΔΔCt) relative to 2D cultures. Significant differences are indicated as * for p < 0.05, ** for p < 0.01, and *** for p < 0.001, one-way ANOVA, N = 2 n = 3). (B) Protein expression characterization of hACh cultured in PCL, PCL/RAD and RAD scaffolds and in 2D monolayer. Western blot results of collagen type I (COL1), II (COL2) and X (COL10) when hACh were maintained in expansion, control and chondrogenic media in the different scaffolds and in 2D monolayer. Actin expression was used as an internal control. Samples were prepared in triplicate. (C) Toluidine blue staining of hACh 3D PCL, PCL/RAD and RAD constructs cultured in expansion, control and chondrogenic medium. Proteoglycan synthesis was qualitatively assessed by toluidine blue staining. Adapted from Recha-Sancho et al. [46].

for RAD scaffold (**Figure 7A**). At protein level, COL2 was only detected in PCL/ RAD and PCL scaffolds under chondrogenic medium (**Figure 7B**). *SOX9* was downregulated in PCL scaffolds in both culture medium and PCL/RAD in expansion medium. Nevertheless, it was maintained similar to 2D levels in PCL/RAD composites under chondrogenic induction and in RAD scaffold (**Figure 7A**). Aggrecan (*ACAN*) gene expression was downregulated in all scaffolds under expansion medium and upregulated in all scaffolds under chondrogenic medium, even though no differences were detected relative to 2D cultures (**Figure 7A**). Hypertrophic markers *COL10* and *RUNX2* were upregulated in some constructs respect to baseline. However, no significant increase for *COL10* was detected in RAD and PCL/ RAD constructs under chondrogenic medium (**Figure 7A**). At protein level, COL10 was detected in all samples (**Figure 7B**).

The production of sulfated glycosaminoglycans was qualitatively assessed by toluidine blue staining. Constructs under chondrogenic medium were the most strongly stained compared to expansion and control medium (**Figure 7C**).

Mechanical properties of the scaffolds alone and hACh 3D constructs were assessed by dynamic mechanical analysis (DMA) at week 4 of culture, and compared to chicken and calf articular cartilage (**Figure 8**). The elastic component (G′, storage modulus) of scaffolds and 3D cultures was significantly lower than values of chicken and calf cartilage. Regarding the viscous component (G″, loss modulus), 3D constructs differed from calf native cartilage, while only PCL cellular scaffolds presented differences with chicken cartilage. All samples presented G′ values higher than G″ values, meaning that the material was more elastic than viscous. Because the complex modulus (G*) is the sum of both components, G* basically corresponds to the elastic component in this case and it presented the same pattern as the storage modulus (G′). Concerning tan(delta), which is the full mechanical response of the material, the scaffolds and cell constructs were closely related to both native cartilages, with exception of RAD constructs in chondrogenic medium, which presented differences with calf cartilage. Moreover, differences were observed between PCL/RAD and RAD constructs under the same medium. The combination of PCL scaffold and RAD hydrogel changed their viscoelastic nature after 4 weeks of culture with hACh, since tan(delta) values of the composite were increased compared to RAD scaffolds alone. This effect was not observed between composites PCL/RAD and PCL scaffold alone.

In the present study we report the chondrogenic capacity of dedifferentiated hACh in a composite scaffold comprising a microscale woven 3D poly (ε-caprolactone) and the peptide nanofiber scaffold RAD16-I. PCL scaffold resembles native cartilage mechanical properties while the RAD16-I hydrogel provides a soft and permissive 3D environment. The expression of chondrogenic markers such
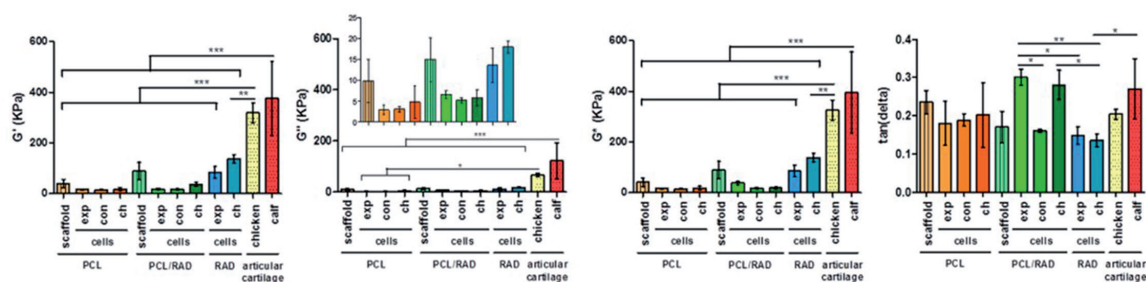

Figure 8.
Mechanical characterization of scaffolds alone and 3D constructs cultured for 4 weeks in expansion, control and chondrogenic medium compared to chicken and calf articular cartilage. hACh cultured in PCL, PCL/ RAD and RAD scaffolds were analyzed for storage modulus (G′), loss modulus (G″), complex modulus (G) and tan(delta). Significant differences are indicated as * for $p < 0.05$, ** for $p < 0.01$, and *** for $p < 0.001$, one-way ANOVA, N = 2 n = 3). Adapted from Recha-Sancho et al. [46].*

as *COL2* and *ACAN* was increased in the presence of RAD16-I peptide (in the composite and alone) compared to 2D cultures (**Figure 7A**). At protein level, different band patterns were detected for COL1, fact that suggests a protein maturation process. Specifically, the scaffolds PCL/RAD and RAD alone under chondrogenic induction, expressed higher levels of the mature COL1, as evidenced by the intensity of the 130 kDa band. Moreover, COL2 was only detected in PCL/RAD and RAD scaffolds under chondrogenic medium, suggesting that the expression of this cartilage-specific protein was due to the presence of RAD16-I hydrogel (**Figure 7B**). GAG production and accumulation was confirmed by toluidine blue staining in constructs under chondrogenic medium (**Figure 7C**). Finally, mechanical characterization showed that at the end of culture, all constructs had a viscoelastic nature (tan delta) similar to native articular cartilage, even though G′ values differed several folds from native cartilage (**Figure 8**). In resume, is clear that the combination of biomaterials to obtain a multi-dimensional composite (microfiber and nanofiber scales) is essential to acquire the best culture conditions for the cells to undergo cartilage lineage differentiation.

4. Conclusions

We report evidences from our previous work which indicates the chondro-inductive capacity of newly developed biomaterials including heparin-, chondroitin sulfate-, decorin-, and poly(ε-caprolactone)-based self-assembling peptide composite scaffolds. In particular, we demonstrated that these biomimetic biomaterials fostered re-differentiation of expanded human articular chondrocytes as well as adipose-derived stem cells into chondrogenic lineage commitment. Moreover, both biological and biomechanical properties obtained of these cartilage substitutes were comparable to natural samples of chicken and calf counterparts. This clearly suggest that these newly class of biomaterials are promising for their future application in reparative and regenerative medicine platforms.

Acknowledgements

Conflict of interest

The authors declare no conflict of interest.

Abbreviations

2D	two dimensional
3D	three dimensional
ADSCs	adipose-derived stem cells
BMSCs	bone marrow mesenchymal stem cells
CS	chondroitin sulfate

CTE	cartilage tissue engineering
Dec	decorin
DMA	dynamic mechanical analysis
ECM	extracellular matrix
GAGs	glycosaminoglycans
G'	storage modulus
G''	loss modulus
G^*	complex modulus
hACh	human articular chondrocytes
HBD	heparin binding domain
Hep	heparin
MSCs	mesenchymal stem cells
PCL	poly(ε-caprolactone)
PGs	proteoglycans
PGA	polyglycolic acid
PLGA	poly(lactic-co-glycolic acid)
PLA	polylactic acid
SAPS	self-assembling peptide scaffolds
SEM	scanning electron microscope

Author details

Nausika Betriu[2] and Carlos E. Semino[1,2*]

1 Tissue Engineering Research Laboratory, Department of Bioengineering, IQS-School of Engineering, Ramon Llull University, Barcelona, Spain

2 Hebe Biolab S.L. C/Can Castellví 27, Barcelona, Spain

*Address all correspondence to: carlos.semino@iqs.url.edu

IntechOpen

References

[1] Chung C, Burdick JA. Engineering cartilage tissue. Advanced Drug Delivery Reviews. 2008;**60**(2):243-262. DOI: 10.1016/j.addr.2007.08.027

[2] Hunziker EB. Articular cartilage repair: Basic science and clinical progress. A review of the current status and prospects. Osteoarthritis and Cartilage. 2002;**10**(6):432-463. DOI: 10.1053/joca.2002.0801

[3] Chiang H, Jiang CC. Repair of articular cartilage dafects: Review and perspectives. Journal of the Formosan Medical Association. 2009;**108**(2):87-101. DOI: 10.1016/S0929-6646(09)60039-5

[4] Castells-sala C, Recha L. Current applications of tissue engineering in biomedicine, Journal of Biochips & Tissue Chips. 2015;**s2**:004. DOI: 10.4172/2153-0777.S2-004

[5] Cucchiarini M, Madry H, Guilak F, Saris DB, Stoddart MJ, Koon Wong M, et al. A vision on the future of articular cartilage repair. European Cells & Materials. 2014;**27**(Suppl):12-16. DOI: 10.22203/eCM

[6] Hubka KM, Dahlin RL, Meretoja VV, Kasper FK, Mikos AG. Enhancing chondrogenic phenotype for cartilage tissue engineering: Monoculture and coculture of articular chondrocytes and mesenchymal stem cells. Tissue Engineering. Part B, Reviews. 2014;**20**(6):641-654. DOI: 10.1089/ten.teb.2014.0034

[7] Pittenger MF, Mackay AM, Beck SC, Jaiswal RK, Douglas R, Mosca JD, et al. Multilineage potential of adult human mesenchymal stem cells. Science. 1999;**284**(5411):143-147. DOI: 10.1126/science.284.5411.143

[8] Darling EM, Athanasiou KA. Rapid phenotypic changes in passaged articular chondrocyte subpopulations. Journal of Orthopaedic Research. 2006;**23**(2):425-432. DOI: 10.1016/j.orthres.2004.08.008

[9] Hong E, Reddi AH. Dedifferentiation and redifferentiation of articular chondrocytes from surface and middle zones: Changes in MICRORNAS-221/-222, -140, and -143/145 expression. Tissue Engineering. Part A. 2012;**19**(7-8):1015-1022. DOI: 10.1089/ten.tea.2012.0055

[10] Griffith LG, Swartz MA. Capturing complex 3D tissue physiology in vitro. Nature Reviews. Molecular Cell Biology. 2006;**7**(3):211-224. DOI: 10.1038/nrm1858

[11] Lee S-H, Shin H. Matrices and scaffolds for delivery of bioactive molecules in bone and cartilage tissue engineering. Advanced Drug Delivery Reviews. 2007;**59**(4):339-359. DOI: 10.1016/j.addr.2007.03.016

[12] Fischbach C, Chen R, Matsumoto T, Schmelzle T, Brugge JS, Polverini PJ, et al. Engineering tumors with 3D scaffolds. Nature Methods. 2007;**4**(10):855-860. DOI: 10.1038/nmeth1085

[13] Horning JL, Sahoo SK, Vijayaraghavalu S, Dimitrijevic S, Vasir JK, Jain TK, et al. 3-D tumor model for in vitro evaluation of anticancer drugs. Molecular Pharmaceutics. 2008;**5**(5):849-862. DOI: 10.1021/mp800047v

[14] Sahoo SK, Panda AK, Labhasetwar V. Characterization of porous PLGA/PLA microparticles as a scaffold for three dimensional growth of breast cancer cells. Biomacromolecules. 2005;**6**(2):1132-1139. DOI: 10.1021/bm0492632

[15] Schneider JP, Pochan DJ, Ozbas B, Rajagopal K, Pakstis L, Kretsinger J.

Responsive hydrogels from the intramolecular folding and self-assembly of a designed peptide. Journal of the American Chemical Society. 2002;**124**(50):15030-15037. DOI: 10.1021/ja027993g

[16] Genové E, Shen C, Zhang S, Semino CE. The effect of functionalized self-assembling peptide scaffolds on human aortic endothelial cell function. Biomaterials. 2005;**26**(16):3341-3351. DOI: 10.1016/j.biomaterials.2004.08.012

[17] Semino CE. Self-assembling peptides: From bio-inspired materials to bone regeneration. Journal of Dental Research. 2008;**87**(7):606-616. DOI: 10.1177/154405910808700710

[18] Semino CE. Can we build artificial stem cell compartments ? 2003;**3**:164-169. DOI: 10.1155/S1110724303208019

[19] Elsa G, Stephanie S, Ana S, Salvador B, Augustinus B, Griffith LG, et al. Functionalized self-assembling peptide hydrogel enhance maintenance of hepatocyte activity in vitro. Journal of Cellular and Molecular Medicine. 2009;**13**(9b):3387-3397. DOI: 10.1111/j.1582-4934.2009.00970.x

[20] Sieminski AL, Semino CE, Gong H, Kamm RD. Primary sequence of ionic self-assembling peptide gels affects endothelial cell adhesion and capillary morphogenesis. Journal of Biomedical Materials Research Part A. 2008;**87**(2):494-504. DOI: 10.1002/jbm.a.31785

[21] Wu J, Marí-Buyé N, Muiños TF, Borrós S, Favia P, Semino CE. Nanometric self-assembling peptide layers maintain adult hepatocyte phenotype in sandwich cultures. Journal of Nanobiotechnology. 2010;**8**(1):29. DOI: 10.1186/1477-3155-8-29

[22] Dégano IR, Quintana L, Vilalta M, Horna D, Rubio N, Borrós S, et al. The effect of self-assembling peptide nanofiber scaffolds on mouse embryonic fibroblast implantation and proliferation. Biomaterials. 2009;**30**(6):1156-1165. DOI: 10.1016/j.biomaterials.2008.11.021

[23] Garreta E, Genové E, Salvador B, Semino CE. Osteogenic differentiation of mouse embryonic stem cells and mouse embryonic fibroblasts in a three-dimensional self-assembling peptide scaffold. Tissue Engineering. 2006;**12**(8):2215-2227. DOI: 10.1089/ten.2006.12.2215

[24] Castells-Sala C, Recha-Sancho L, Llucià-Valldeperas A, Soler-Botija C, Bayes-Genis A, Semino CE. Three-dimensional cultures of human subcutaneous adipose tissue-derived progenitor cells based on RAD16-I self-assembling peptide. Tissue Engineering. Part C, Methods. 2016;**22**(2):ten.tec.2015.0270. DOI: 10.1089/ten.tec.2015.0270

[25] Fernández-Muiños T, Recha-Sancho L, López-Chicón P, Castells-Sala C, Mata A, Semino CE. Bimolecular based heparin and self-assembling hydrogel for tissue engineering applications. Acta Biomaterialia. 2015;**16**(1):35-48. DOI: 10.1016/j.actbio.2015.01.008

[26] Chen W-C, Yao C-L, Chu I-M, Wei Y-H. Compare the effects of chondrogenesis by culture of human mesenchymal stem cells with various type of the chondroitin sulfate C. Journal of Bioscience and Bioengineering. 2011;**111**(2):226-231. DOI: 10.1016/j.jbiosc.2010.10.002

[27] Seidler DG, Dreier R. Decorin and its galactosaminoglycan chain: Extracellular regulator of cellular function? IUBMB Life. 2008;**60**(11):729-733. DOI: 10.1002/iub.115

[28] Trowbridge JM, Gallo RL. Dermatan sulfate: New functions from an old

glycosaminoglycan. Glycobiology. 2002;**12**(9):117R-125R. DOI: 10.1093/glycob/cwf066

[29] Moutos FT, Freed LE, Guilak F. A biomimetic three-dimensional woven composite scaffold for functional tissue engineering of cartilage. Nature Materials. 2007;**6**:162. DOI: 10.1038/nmat1822

[30] Huang M-H, Li S, Hutmacher DW, Coudane J, Vert M. Degradation characteristics of poly(ϵ-caprolactone)-based copolymers and blends. Journal of Applied Polymer Science. 2006;**102**(2):1681-1687. DOI: 10.1002/app.24196

[31] Rohner D, Hutmacher DW, Cheng TK, Oberholzer M, Hammer B. In vivo efficacy of bone-marrow-coated polycaprolactone scaffolds for the reconstruction of orbital defects in the pig. Journal of Biomedical Materials Research Part B: Applied Biomaterials. 2003;**66B**(2):574-580. DOI: 10.1002/jbm.b.10037

[32] Freed LE, Engelmayr GC, Borenstein JT, Moutos FT, Guilak F. Advanced material strategies for tissue engineering scaffolds. Advanced Materials. 2009;**21**(32-33):3410-3418. DOI: 10.1002/adma.200900303

[33] Baugé C, Girard N, Lhuissier E, Bazille C, Boumediene K. Regulation and role of TGFβ signaling pathway in aging and osteoarthritis joints. Aging and Disease. 2014;**5**(6):394-405. DOI: 10.14336/AD.2014.0500394

[34] Cals FLJ, Hellingman CA, Koevoet W, Baatenburg de Jong RJ, van Osch GJVM. Effects of transforming growth factor-β subtypes on in vitro cartilage production and mineralization of human bone marrow stromal-derived mesenchymal stem cells. Journal of Tissue Engineering and Regenerative Medicine. 2011;**6**(1):68-76. DOI: 10.1002/term.399

[35] Chen WH, Lai MT, Wu ATH, Wu CC, Gelovani JG, Lin CT, et al. In vitro stage-specific chondrogenesis of mesenchymal stem cells committed to chondrocytes. Arthritis and Rheumatism. 2009;**60**(2):450-459. DOI: 10.1002/art.24265

[36] Chung C, Burdick JA. Engineering cartilage tissue. Advanced Drug Delivery Reviews. 2008;**60**(2):243-262. DOI: 10.1016/j.addr.2007.08.027

[37] Awad HA, Wickham MQ, Leddy HA, Gimble JM, Guilak F. Chondrogenic differentiation of adipose-derived adult stem cells in agarose, alginate, and gelatin scaffolds. Biomaterials. 2004;**25**(16):3211-3222. DOI: 10.1016/j.biomaterials.2003.10.045

[38] Masuoka K, Asazuma T, Hattori H, et al. Tissue engineering of articular cartilage with autologous cultured adipose tissue-derived stromal cells using atelocollagen honeycomb-shaped scaffold with a membrane sealing in rabbits. Journal of Biomedical Materials Research. Part B, Applied Biomaterials. 2006;**79**(1):25-34. DOI: 10.1002/jbmb

[39] Sechriest VF, Miao YJ, Niyibizi C, Westerhausen-Larson A, Matthew HW, Evans CH, et al. GAG-augmented polysaccharide hydrogel: A novel biocompatible and biodegradable material to support chondrogenesis. Journal of Biomedical Materials Research. 2000;**49**(4):534-541. DOI: 10.1002/(SICI)1097-4636(20000315)49:4<534::AID-JBM12>3.0.CO;2-#

[40] Varghese S, Hwang NS, Canver AC, Theprungsirikul P, Lin DW, Elisseeff J. Chondroitin sulfate based niches for chondrogenic differentiation of mesenchymal stem cells. Matrix Biology. 2008;**27**(1):12-21. DOI: 10.1016/j.matbio.2007.07.002

[41] Mullen LM, Best SM, Ghose S, Wardale J, Rushton N, Cameron RE.

Bioactive IGF-1 release from collagen–GAG scaffold to enhance cartilage repair in vitro. Journal of Materials Science. Materials in Medicine. 2015;**26**(1):1-8. DOI: 10.1007/s10856-014-5325-y

[42] Recha-Sancho L, Semino CE. Chondroitin sulfate- and decorin-based self-Assembling scaffolds for cartilage tissue engineering. PLoS One. 2016;**11**(6):1-23. DOI: 10.1371/journal.pone.0157603

[43] Valonen PK, Moutos FT, Kusanagi A, Moretti MG, Diekman BO, Welter JF, et al. In vitro generation of mechanically functional cartilage grafts based on adult human stem cells and 3D-woven poly (ε-caprolactone) scaffolds. Biomaterials. 2010;**31**(8):2193-2200. DOI: 10.1016/j.biomaterials.2009.11.092

[44] Moutos FT, Guilak F. Functional properties of cell-seeded three-dimensionally woven poly (ε-caprolactone) scaffolds for cartilage tissue engineering. Tissue Engineering. Part A. 2009;**16**(4):1291-1301. DOI: 10.1089/ten.tea.2009.0480

[45] Liao I-C, Moutos FT, Estes BT, Zhao X, Guilak F. Composite three-dimensional woven scaffolds with interpenetrating network hydrogels to create functional synthetic articular cartilage. Advanced Functional Materials. 2013;**23**(47):5833-5839. DOI: 10.1002/adfm.201300483

[46] Recha-Sancho L, Moutos FT, Abellà J, Guilak F, Semino CE. Dedifferentiated human articular chondrocytes redifferentiate to a cartilage-like tissue phenotype in a poly(ε-caprolactone)/Self-assembling peptide composite scaffold. Materials. 2016;**9**(6). DOI: 10.3390/ma9060472